Zhou, Chen, C., Wang, M., & Khandelwal, M. (2021). Proposing a novel comprehensive evaluation model for the coal burst liability in underground coal mines considering uncertainty factors*. International Journal of Mining Science and Technology, 31*(5), 799–812.

Available online: https://doi.org/10.1016/j.ijmst.2021.07.011

International Journal of Mining Science and Technology 31 (2021) 799–812

Contents lists available at ScienceDirect

International Journal of Mining Science and Technology

journal homepage: www.elsevier.com/locate/ijmst

Proposing a novel comprehensive evaluation model for the coal burst liability in underground coal mines considering uncertainty factors

Jian Zhou [a,*], Chao Chen [a], Mingzheng Wang [b,*], Manoj Khandelwal [c]

[a] School of Resources and Safety Engineering, Central South University, Changsha 410083, China
[b] Bharti School of Engineering, Laurentian University, Sudbury, Ontario, Canada
[c] School of Engineering, Information Technology and Physical Sciences, Federation University Australia, Ballarat, Australia

ARTICLE INFO

Article history:
Received 31 January 2021
Received in revised form 18 May 2021
Accepted 29 July 2021
Available online 7 August 2021

Keywords:
Coal burst liability (*CBL*)
Unascertained measurement (*UM*)
Analysis hierarchy process
Information entropy
Synthetic weights
Comprehensive evaluation

ABSTRACT

Coal burst is a severe hazard that can result in fatalities and damage of facilities in underground coal mines. To address this issue, a robust unascertained combination model is proposed to study the coal burst hazard based on an updated database. Four assessment indexes are used in the model, which are the dynamic failure duration (*DT*), elastic energy index (W_{ET}), impact energy index (K_E) and uniaxial compressive strength (R_C). Four membership functions, including linear (*L*), parabolic (*P*), *S* and Weibull (*W*) functions, are proposed to measure the uncertainty level of individual index. The corresponding weights are determined through information entropy (*EN*), analysis hierarchy process (*AHP*) and synthetic weights (*CW*). Simultaneously, the classification criteria, including unascertained cluster (*UC*) and credible identification principle (*CIP*), are analyzed. The combination algorithm, consisting of *P* function, *CW* and *CIP* (*P-CW-CIP*), is selected as the optimal classification model in function of theory analysis and to train the samples. Ultimately, the established ensemble model is further validated through test samples with 100% accuracy. The results reveal that the hybrid model has a great potential in the coal burst hazard evaluation in underground coal mines.

1. Introduction

Coal resources, which are known as the food of industry, still play a major role in industry, such as electricity, building materials and chemical engineering. The valuable and non-renewable resources are being exhausted and depleted due to uncontrolled exploitation. And the tendency to extract solid mineral resources at greater depth is inevitable [1]. However, the geological conditions and mechanical properties of coal mass are complex at greater depth [2], which means that the coal burst control has been a challenging mission [3].

Coal burst is defined as the violent ejection of coal/rock from the work face with a sudden release of accumulated energy [4]. In most cases, the coal burst is associated with the mining disturbance, which can cause catastrophic damage to personnel and equipment [5], as shown in Fig. 1. Thus, many scholars [6–15] carried out studies on the issues, including on-site monitoring techniques [16] and assessment methods. For example, some scholars employed mathematical analysis [17] and fuzzy comprehensive evaluation [18] to assess the coal burst liability (*CBL*) according to the spatial distribution characteristics of *AE* events. Various destress methodologies, such as destress blasting and water infusions, are used to mitigate the degree of coal burst. Yardimci and Karakus [19] assessed the effect of destress blasting according to the location and roof stability. Guo et al. [20] investigated the relation between the coal burst potential indexes (i.e., R_C, W_{ET}, K_E and *DT*) and the saturation time of coal mass in order to explore the effect of water infusion on coal burst proneness. They found that the tendency of coal burst has a negative correlation with the saturation time. In recent years, many rock burst studies are carried out [21–29], which has been getting wider attention in the geosciences. The investigation of coal burst prevention would be able to provide valuable strategies for other rock mass engineering, given the burst control principle is similar for rock and coal masses [30]. Thus, it is necessary to explore more efficient and effective methods for coal burst control. However, the disturbance of on-site tests may trigger coal burst hazards, which puts the operators into a dangerous environment. As for laboratory test, the test process is complicated and time-consuming [31]. Furthermore, the properties of rock specimen and rock mass are largely different, which is unable to reflect the actual conditions absolutely through the indoor tests. Currently, the Chinese national standard (*GB*) [32],

* Corresponding authors.
E-mail addresses: csujzhou@hotmail.com, j.zhou@csu.edu.cn (J. Zhou), mwang3@laurentian.ca (M. Wang).

https://doi.org/10.1016/j.ijmst.2021.07.011
2095-2686/

(a) The longwall panel before coal burst (b) The longwall panel after coal burst (c) The tailgate before coal burst (d) The tailgate after coal burst

Fig. 1. Destruction caused by severe coal burst in underground coal mines [38,39].

namely four parameters, (i.e., R_C, W_{ET}, K_E and DT) is a commonly used method for identifying the coal burst propensity in China, but the criterion is not capable and applicable in some complex situations, where the indexes belong to different grades separately.In view of the aforementioned analysis, it seems that evaluation of *CBL* with reliable mathematical models is available with the development and application of artificial intelligence [33–36,101–103] in mining engineering, e.g., principal component analysis (PCA) [37], but, the performance of these models need to be further validated through an inspired amount of data. The key objective of this research is to propose a new combination algorithm based on an unascertained measurement model, which has been accepted in various engineering fields for a highly-efficient and reliable method through the gathered database. The key contributions of this research are summarized as follows: this work incorporates an updated database including 121 coal burst case studies to assess and study this issue. The evaluation with non-linear membership functions are rarely considered in unascertained measurement theory in previous work. Two novel membership functions, i.e., *S* and *W* functions, are added to support the non-linear evaluation. Meanwhile, the evaluation performance of multiple ensemble models consisting of different membership functions and weights are analyzed. Ultimately, the proposed uncertainty model is capable of making up for the deficiencies of *GB* in terms of the evaluation accuracy.

2. Description of unascertained measurement theory

Unascertained information is seen as a weak uncertainty that can be interpreted via subjective probability or membership functions [40]. For the object to be evaluated, n objects constitute the sample set ψ={ψ_1, ψ_2, …, ψ_n}. For individual samples ψ_o=$(1 \le o \le n)$, the characteristics can be extracted by many quantitative and qualitative factors. Then, m characteristics are performed to describe the specimen attribute composed of an index set Φ={ϕ_1, ϕ_2, …, ϕ_m}$(1 \le p \le m)$. Q_{op}(o = 1, 2, …, n; and p = 1, 2, …, m) is the quantified value of pth index. There are G possible evaluation classes for each object, and they are stored in evaluation space Λ={ξ_1, ξ_2, …, ξ_G}. The evaluation space Λ can be considered as an ordered partition, while the grade vector ξ_q(q = 1, 2, …, G) meets the condition $\xi_1 > \xi_2 > \ldots > \xi_G$ or $\xi_1 < \xi_2 < \ldots < \xi_G$.

2.1. Quantifying the uncertainty correlation using membership functions

The $D_o^{pq}=(D(Q_{op} \in \xi_q))$($o$ = 1, 2, …, n; p = 1, 2, …, m; and q = 1, 2, …, G) is supposed as the single index vector, which represents the level of index ϕ_p belonging to grade ξ_q. The multiple-index measurement matrix was calculated based on the sample characteristic matrix $(Q_{op})_{n\times m}$ and related membership functions (i.e., straight line, parabolic curve, *S* curve and Weibull curve). The principle of different membership methodologies is shown in Eqs. (1)–(4) and Fig. 2. There are three rules [41,42], including non-negative (Eq. (5)), convergent (Eq. (6)) and additive principle (Eq. (7)), that must be satisfied for single index measurement vectors, which can validate the results.

$$\begin{cases} D_l(x) = \begin{cases} \frac{\Delta_{l+1}-x}{\Delta_{l+1}-\Delta_l} \; (\Delta_l < x \leqslant \Delta_{l+1}) \\ 0 \quad (x > \Delta_{l+1}) \end{cases} \\ D_{l+1}(x) = \begin{cases} 0 \; (x \leqslant \Delta_l) \\ \frac{x-\Delta_l}{\Delta_{l+1}-\Delta_l} \; (\Delta_l < x \leqslant \Delta_{l+1}) \end{cases} \end{cases} \tag{1}$$

$$\begin{cases} D_l(x) = \begin{cases} 1-\left(\frac{x-\Delta_l}{\Delta_{l+1}-\Delta_l}\right)^2 \; (\Delta_l < x \leqslant \Delta_{l+1}) \\ 0 \; (x > \Delta_{l+1}) \end{cases} \\ D_{l+1}(x) = \begin{cases} 0 \; (x \leqslant \Delta_{l+1}) \\ \left(\frac{x-\Delta_l}{\Delta_{l+1}-\Delta_l}\right)^2 \; (\Delta_l < x \leqslant \Delta_{l+1}) \end{cases} \end{cases} \tag{2}$$

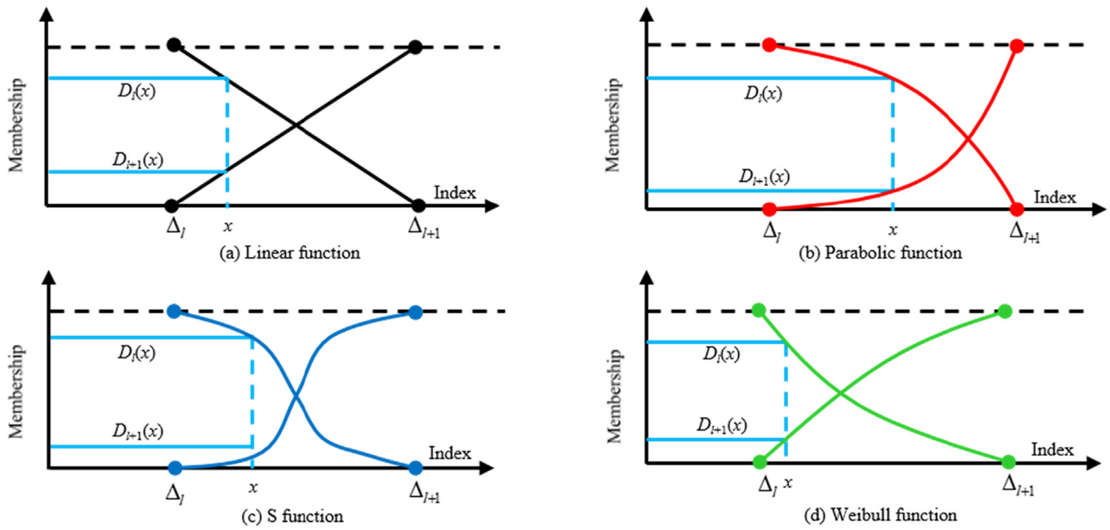

Fig. 2. Schematic diagram of different membership functions.

$$\left\{\begin{array}{l} D_l = \left\{\begin{array}{ll} 1 & (x \leqslant \Delta_l) \\ 1-2\left(\frac{x-\Delta_l}{\Delta_{l+1}-\Delta_l}\right)^2 & \left(\Delta_l < x \leqslant \frac{\Delta_l+\Delta_{l+1}}{2}\right) \\ 2\left(\frac{x-\Delta_{l+1}}{\Delta_{l+1}-\Delta_l}\right)^2 & \left(\frac{\Delta_l+\Delta_{l+1}}{2} < x < \Delta_{l+1}\right) \\ 0 & (x \geqslant \Delta_{l+1}) \end{array}\right. \\ D_{l+1} = \left\{\begin{array}{ll} 0 & (x \leqslant \Delta_l) \\ 2\left(\frac{x-\Delta_l}{\Delta_{l+1}-\Delta_l}\right)^2 & \left(\Delta_l < x \leqslant \frac{\Delta_l+\Delta_{l+1}}{2}\right) \\ 1-2\left(\frac{x-\Delta_{l+1}}{\Delta_{l+1}-\Delta_l}\right)^2 & \left(\frac{\Delta_l+\Delta_{l+1}}{2} < x < \Delta_{l+1}\right) \\ 1 & (x \geqslant \Delta_{l+1}) \end{array}\right. \end{array}\right. \tag{3}$$

$$\left\{\begin{array}{l} D_l(x) = \left\{\begin{array}{l} 1-\frac{e}{e-1}\left(1-\exp\left(-\left(\frac{x-\Delta_l}{\Delta_{l+1}-\Delta_l}\right)\right)\right)(\Delta_l < x \leqslant \Delta_{l+1}) \\ 0 \quad (x > \Delta_{l+1}) \end{array}\right. \\ D_{l+1}(x) = \left\{\begin{array}{l} 0 \quad (x \leqslant \Delta_l) \\ \frac{e}{e-1}\left(1-\exp\left(-\left(\frac{x-\Delta_l}{\Delta_{l+1}-\Delta_l}\right)\right)\right)(\Delta_l < x \leqslant \Delta_{l+1}) \end{array}\right. \end{array}\right. \tag{4}$$

$$(1)\ \text{Non–negativity}\ 0 \le D(Q_{op} \in \xi_q) \le 1 \tag{5}$$

$$(2)\ \text{Normalization}\, D(Q_{op} \in \Lambda) = 1 \tag{6}$$

$$(3)\ \text{Additivity}\, D\left[Q_{op} \in \bigcup_{r=1}^{q} \xi_r\right] = \sum_{r=1}^{q} Q_{op} \in \xi_r (q = 1, 2, \cdots, G) \tag{7}$$

2.2. Objective weights calculation using entropy theory

The index weights in evaluation space are needed to distinguish as the multiple-index measurement matrices were constructed. The information entropy, as one of the objectivity weights, which is the term originating from thermodynamics, reflects the degree of information disorder. The weight distribution was calculated, shown in Eqs. (8) and (9).

$$\zeta_p = -\frac{1}{\ln G}\sum_{q=1}^{G} D_o^{pq} \ln D_o^{pq} (D_o^{pq} \neq 0; 1 \leqslant o \leqslant n; 1 \leqslant p \leqslant m; 1 \leqslant q \leqslant G) \tag{8}$$

$$\left(\varpi_1^{obj}\right)_p = \frac{1-\zeta_p}{\sum_{p=1}^{m}(1-\zeta_p)} \tag{9}$$

where $\zeta_p(p = 1, 2, \ldots, m)$ is the entropy value, from which the objective weight vector $({\varpi_1}^{obj})_p$ can be obtained.

2.3. Subjective weights calculation using the analysis hierarchy process (AHP)

AHP proposed by Saaty [43] divides the evaluation objects into goal hierarchy, criterion hierarchy and index hierarchy. In this work, the index weights are calculated based on the designer's knowledge. The superiority of this method is that it can adjust the weight assignment through the pairwise comparison matrix compared to the objective weight. A situation where the calculated weights are far from the actual conditions can be largely avoided [44].

2.3.1. Establishment of pairwise comparison matrix

For index set $\Phi=\{\phi_1, \phi_2, \ldots, \phi_m\}$, supposing $c_{ij}(1 \le i \le m; 1 \le j \le m)$ is the score of index ϕ_i to ϕ_j, which is the significance level in designer's expectation. On the contrary, c_{ji} is the value of index ϕ_j to ϕ_i, and $c_{ij}c_{ji} = 1$. Then, the pairwise comparison matrix is constructed as presented in Eq. (10).

$$C_{m\times m} = \begin{bmatrix} c_{11} & c_{12} & \cdots & c_{1m} \\ c_{21} & c_{22} & \cdots & c_{2m} \\ \vdots & \vdots & \ddots & \vdots \\ c_{m1} & c_{m2} & \cdots & c_{mm} \end{bmatrix} \tag{10}$$

2.3.2. Computation of weight vectors and consistency check

According to the pairwise comparison matrix $C_{m\times m}$, the maximum eigenvalue $\lambda_{\max}$ and related eigenvector can be achieved easily. Then, the consistency check is used to examine the feasibility of index weights that we assigned. The process of checking is shown in Eqs. (11) and (12).

$$CI = \frac{\lambda_{\max} - m}{m-1} \tag{11}$$

$$CR = \frac{CI}{RI} \tag{12}$$

The consistency index (CI) is calculated by Eq. (11) and m is the dimension of the comparison matrix. To check the criterion, consistency ratio (CR) is obtained via CI to RI. The comparison matrix is reasonable and the corresponding eigenvectors can be regarded

Table 1
Basis to select the value of *RI*.

m	1	2	3	4	5	6	7	8	9	10	11
RI	0	0	0.58	0.90	1.12	1.24	1.32	1.41	1.45	1.49	1.51

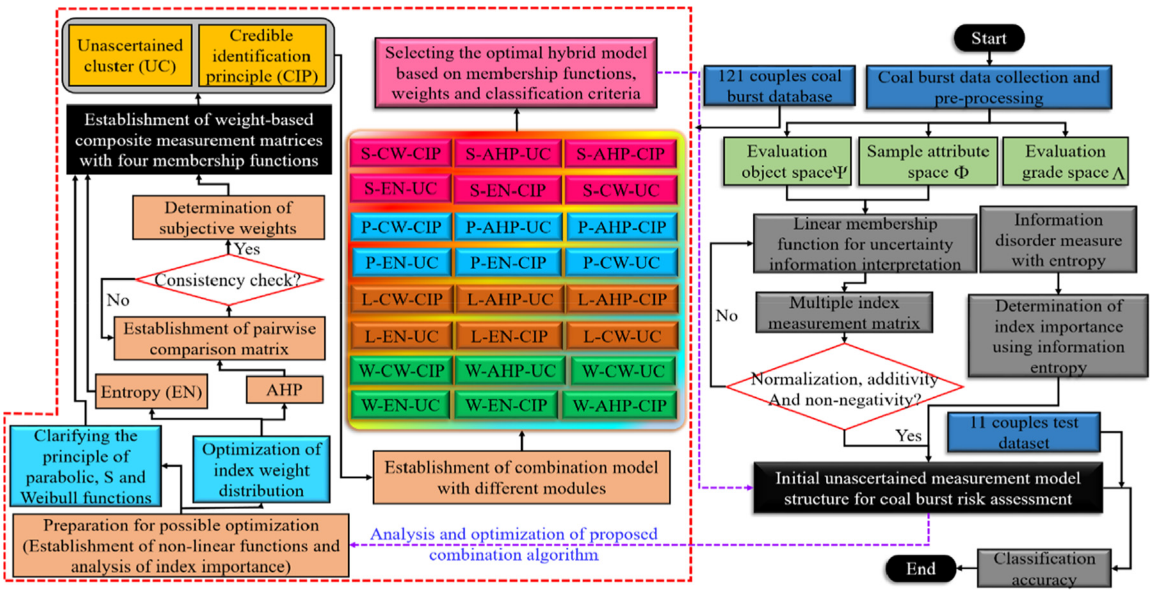

Fig. 3. Technique routine for *CBL* evaluation using combination algorithm.

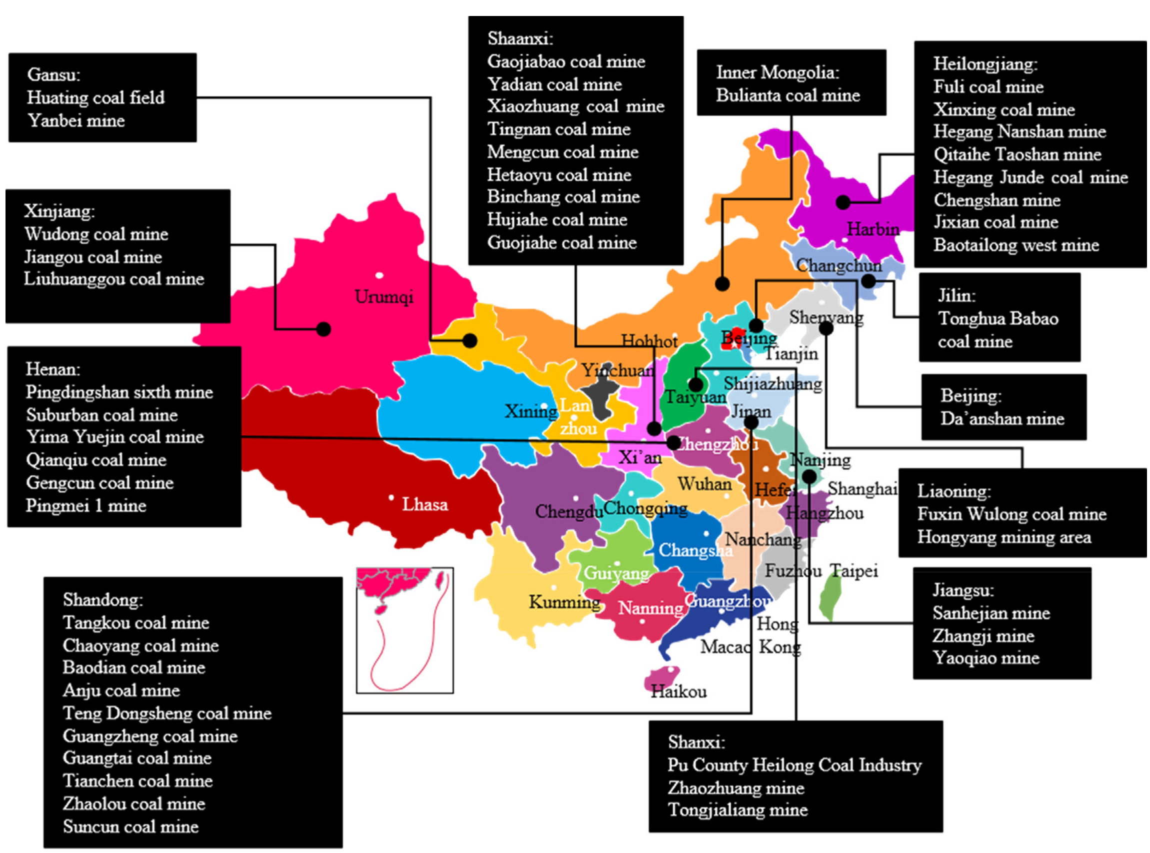

Fig. 4. Distribution of the mines corresponding to the sample set.

Table 2
Coal burst database used for establishing comprehensive evaluation model.

No.	Case	CBL parameter				Grade	Reference
		DT (ms)	W_{ET}	K_E	R_C (MPa)		
1	Tonghua Babao coal mine	973	2.7	1.8	5.9	1	Luo et al. (2020) [50]
2	Pingdingshan sixth mine	357	2.9	4.6	11.5	2	
3	Wulong coal mine	49	4.6	6	16.5	3	
4	Gaojiabao coal mine #4	291	12.5	3.1	19.3	3	Wang et al. (2019) [51]
5	Tangkou coal mine #3	72	13.2	2.4	19.3	3	
6	#10 coal in a mine	423	5.3	2.6	27.3	3	
7	Binchang coal mine 4 lower coal	112	19.4	4.3	26.9	3	
8	Fuli coal mine 22 coal	147	13.3	4.8	30.3	3	
9	Bulianta coal mine	50	8.5	65.9	31.7	3	
10	60 coal in the sixth mining area of Xinxing coal mine	459	10	9.9	9.8	2	
11	Chaoyang coal mine 3100 mining area	23	49	5.1	4.6	3	
12	3 coal in Baodian coal mine	42	21.9	5.4	26.6	3	
13	Wudong coal mine B6 coal	254	1.6	1.5	12.6	2	
14	Bulianta coal mine (gas pressure 0)	49.667	8.472	65.921	31.661	3	Gao et al. (2018) [52]
15	Bulianta coal mine (gas pressure 1)	148.667	2.036	7.368	23.954	3	
16	Bulianta coal mine (gas pressure 2)	321.667	1.246	2.478	13.052	2	
17	Yadian coal mine 1 coal	707	12.15	2.8	13.67	2	Pan et al. (2019) [53]
18	Xiaozhuang coal mine #4	208.8	7.32	1.53	13.23	2	
19	Tingnan coal mine 4 coal (the second panel district)	278	10.28	3.39	16.68	3	
20	Upper stratification of 4 coal in Gaojiabao coal mine	278.4	13.36	3.2	20.47	3	
21	Layer 4 of Gaojiabao coal mine	303.4	11.54	2.98	18.18	3	
22	Upper layer of 4 coal in Mengcun coal mine	72	13.35	6.2	19.37	3	
23	Lower layer of 4 coal in Mengcun coal mine	112	19.35	4.26	26.88	3	
24	Layer 8 in Hetaoyu coal mine	613	3.59	3.78	24	2	
25	Upper stratification of 4 coal in Hujiahe coal mine	39.8	6.49	7.73	24.27	3	Wu et al. (2015) [54]
26	Hujiahe coal mine 4 coal lower layer	34.4	4.45	12.57	24.35	3	
27	B1 + 2 coal seam of Jiangou coal mine	285	1.91	2.02	10.1	2	Cao et al. (2019) [55]
28	B3 + 6 coal seam of Jiangou coal mine	254	1.46	1.59	12.64	2	
29	Liuhuanggou coal mine	31.5	5.6	12	35.4	3	Zhu et al. (2019) [56]
30	Anju coal mine 3 coal	161.4	3.382	2.253	13.79	2	Wang et al. (2019) [57]
31	–	133592	3.93	1.04	4.56	1	Wang et al. (2019) [58]
32	–	10702	5.32	12.21	15.17	3	
33	Huating coalfield	45	12.3	12.57	18.77	3	Li et al. (2016) [59]
34		73	2.96	19.37	14.67	3	
35		158	5.1	6.13	13	3	
36		60	2.93	13.51	14.32	3	
37		33	10.28	9.84	12.09	3	
38		141	5.12	5.6	10.56	3	
39		82	4.78	10.18	13.9	3	
40		20	9.43	8.72	16.5	3	
41		105	7.71	4.21	13.89	3	
42	South of 7 coal seam in Sanhejian mine	54	19.63	1.29	17.25	3	Guo (2017) [60]
43	South of 7 coal seam in Sanhejian mine	46.2	14.51	18.78	34.32	3	
44	Sanhejian mine 9 layers of coal 9108	12	3.6	2.3	37.7	3	
45	South of 9 coal seams in Sanhejian mine	70	7.83	3.38	20.76	3	
46	South of 9 coal seams in Sanhejian mine	51.25	5.74	1.8	18.5	3	
47	237 working face of Hegang Nanshan mine	1414	3.29	2.38	5.26	1	
48	Da'anshan mine 7 slots coal	138.4	0.97	3.54	9.97	2	
49	Xuzhou Zhangji mine 9612 working face	52.5	6.62	4.32	9.52	2	
50	Qitaihe Taoshan mine 79 coal	50.35	6.71	4.52	11.78	2	
51	Hegang Junde mine 17 coal	346	11.3	6.45	15.24	3	
52	5 layers of coal in Yanbei	248.57	2.15	1.84	12.03	2	
53	9 and 10 coal seams	375	2.1	1.93	11.43	2	Li (2011) [61]
54	15 coal seam	137	5.28	4.15	13.75	2	
55	16 and 17 coal seams	258	2.01	2.05	12.49	2	
56	20 coal seam	185	2.78	3.26	13.28	2	
57	Puxian Heilong Coal Industry	402	5.332	2.632	27.279	3	Bai (2018) [62]
58	Chengjiao coal mine No. 2 coal seam	306	5.91	2.48	8.86	2	Su (2013) [63]
59	Chengshan mine #25	284	3.96	1.84	10.48	2	Li et al. (2013) [64]
60	Yuejin coal mine	351	2.63	1.64	12.98	2	Song et al. (2014) [65]
61	Tengdong Shengjian coal mine #1 coal seam	37	5.33	5.01	15.56	3	Wan (2015) [66]
62	Tengdong Shengjian coal mine #2 coal seam	91	4.36	3.89	14.4	2	
63	Tengdong Shengjian coal mine #3 coal seam	144	3.46	3.21	13.35	2	
64	Tengdong Shengjian coal mine #4 coal seam	113	2.78	2.71	12.46	2	
65	Tengdong Shengjian coal mine #5 coal seam	149	2.58	2.37	11.61	2	
66	–	362.8	6.02	1.34	8.61	2	Gong et al. (2015) [67]
67	Hongyang coalfield #12	252	3.11	1.93	6.51	2	Wang et al. (2016) [68]
68	8 coal seam	100	6.41	2.76	17.15	2	Su et al. (2014) [69]
69	16 and 17 coal seam	24	4	2.85	23.85	3	
70	15 coal seam	301	3.84	2.47	10.2	2	
71	9 and 10 coal seam	92	4.3	4.53	14.65	2	
72	Qianqiu coal mine No. 2 seam top coal	300	2.76	2.74	11.76	2	Li (2014)[70]
73	Qianqiu coal mine No. 2 seam bottom coal	224	6.44	6.32	18.61	3	

(*continued on next page*)

Table 2 (*continued*)

No.	Case	*CBL* parameter				Grade	Reference
		DT (ms)	W_{ET}	K_E	R_C (MPa)		
74	Yaoqiao mine 7 coal	19	7.86	13.667	9.72	3	Zhang et al. (2015) [71]
75	Xinxing mine sixth mining area	41.2	11.91	11.76	5.489	3	Shu et al. (2014) [72]
76	A mine in Xinjiang	44.5	4.34	5.99	22.63	3	Yang (2013) [73]
77	A mine in Shandong	139.8	3.19	3.34	13.29	2	
78	A mine in Inner Mongolia	722	1.9	1.54	7.05	1	
79	Shandong #1	760	2.13	1.17	5.92	1	Xu et al. (2013) [74]
80	Inner Mongolia #2	260	1.88	1.67	12.87	2	
81	Heilongjiang #3	189	6.05	6.49	18.64	3	
82	Guangzhong coal mine	260	2.4	0.76	4.27	1	Li et al. (2014) [75]
83	Guangtai coal mine	212	4.34	0.88	7.31	2	
84	Guojiahe coal mine	267	12.4	0.87	24.77	3	
85	Yuejin coal mine	65.89	10.42	6.3	28.6	3	Guo (2016) [76]
86	Zhaozhuang coal mine #3	196.2	1.93	1.078	8.903	2	Tong (2014) [77]
87	Jixian mine Q1	288	1.63	2.34	15.37	2	Xing (2014) [78]
88	Jixian mine Q2	239	1.4	2.03	11.14	2	
89	–	48	8.06	9.4	10.58	3	Li (2013) [79]
90	1 coal	34	5.15	6.5	17.35	3	Wang (2013) [80]
91	2 coal	255	3.4	3.7	11.15	2	
92	3 coal	725	1.58	1.4	5.36	1	
93	–	3492	6.3	9.75	22.44	3	Song et al. (2018)[81]
94	–	18150	2.5	2.58	7.07	2	
95	–	31325	0.2	1.37	2.04	1	
96	Upper stratification	167	17.603	15.682	22.597	3	Jiang et al. (2018) [82]
97	Lower stratification	69.2	12.522	35.723	33.907	3	
98	3 coal	90	5.27	3.18	18.39	3	Zhan (2018) [83]
99	7609 working face of Gengcun coal mine (natural)	254	3	1.94	7.31	2	Xiao et al. (2018) [84]
100	7609 working face of Gengcun coal mine (saturated with water)	500	1.9	1.63	5.71	2	
101	Baotailong west mine district 26a	750.3	8.19	1.36	9.52	3	Shen and Jiang (2016) [85]
102	Baotailong west mine district 26b	421.8	22.67	1.39	17.4	3	
103	Tengdong coal mine 3 coal	43.2	14.6	11.8	34.06	3	Chen (2015) [86]
104	Tianchen coal mine 322 face	360	2.25	13.84	10	2	Liu et al. (2014) [87]
105	3 coal in a mine	362.8	6.02	1.34	8.61	2	Zhu (2013) [88]
106	Tongjialiang mine	5.7	9.1	6.48	14.5	3	Liu (2011) [89]
107	Huating coal mine 5 middle bed coal	38	14.57	17.46	22.59	3	Wang (2011) [90]
108	Zhaolou coal mine #3 (upper)	42	7.39	5.67	20.5	3	Jiang et al. (2010) [91]
109	Zhaolou coal mine #3	45	5.24	4.96	18.54	3	
110	Zhaolou coal mine #3 (lower)	49	8.12	10.63	25.9	3	
111	#6 coal seam of Pingmei mine	1149	3.39	3.45	14.38	2	Jiao (2010) [92]
112	Suncun mine #1	172	4	1.58	13.17	2	Guo et al. (2003) [93]
113	Chaoyang coal mine	49	5.09	4.59	23.41	3	Li (2008) [94]
114	Yanbei coal mine LW250205	140	6.44	9.51	21	3	Cai et al. (2016) [37]
115	Yanbei coal mine LW250205	109	5.13	2.19	14.57	2	
116	Yanbei coal mine LW250205	141	14.74	6.92	14.34	3	
117	Yanbei coal mine LW250205	250	3.86	3.15	4.33	2	
118	Yanbei coal mine LW250205	141	13.4	2.47	16.55	3	
119	Yanbei coal mine LW250205	250	4.69	2.77	9.17	2	
120	Yanbei coal mine LW250205	31	16.17	12.17	10.14	3	
121	Yanbei coal mine LW250205	203	10.03	4.11	20.37	3	

Notes: – indicates the sample information was removed by authors; and 1, 2 and 3 are denoted as none, weak and strong.

as the index weights $(\varpi_2{}^{sbj})_p$ after normalization as *CR* < 0.1, otherwise, the comparison matrix needs to be reconsidered. The values of *RI* [45] are shown in Table 1.

2.4. Synthetic weights

The synthetic weights ω_p is proposed to combine the data characteristic and subjective judgment to increase the feasibility of weight assignment, which can incorporate the objectivity and rich experience simultaneously from the aforementioned weight methods (Eq. (13)).

$$\omega_p = \frac{\left(\varpi_1^{obj}\right)_p\left(\varpi_2^{sbj}\right)_p}{\sum_{k=1}^{m}\left(\varpi_1^{obj}\right)_k\left(\varpi_2^{sbj}\right)_k}(p = 1, 2, \cdots, m) \tag{13}$$

2.5. Calculation of composite measurement vectors

Index measurement vector D_o^{pq} determines the level of index ϕ_p belonging to grade ξ_q. Comprehensive evaluations are usually achieved based on the specimen, which means that the degree of sample ψ_o belonging to grade ξ_q needs to be clear. Thus, composite measurement vectors δ_{oq} are calculated in function of the multiple index measurement matrix and related weights (Eq. (14)).

$$\delta_{oq} = \sum_{p=1}^{m}\omega_p D_o^{pq}(o = 1, 2, \cdots, n; p = 1, 2, \cdots, m; q = 1, 2, \cdots, G) \tag{14}$$

2.6. Principle and priority of credible identification

Given that the evaluation space Λ is the ordered partition, thus, credible recognition criterion λ is employed in this work, which has better performance than the conventional identification methodologies, such as maximum measurement principle. The grade $\Lambda_q(1 \le q \le G)$ is considered as the assessment result that satisfies $\sum\xi_q \ge \lambda$ (Eq. (15)). Generally, 0.5 $\le \lambda \le$ 1 and it is common that λ = 0.6–0.7 [46–49].

$$\Lambda_q = min\{q : \sum \xi_r \ge \lambda, 1 \le r \le G\} \tag{15}$$

Assuming that the grade value ξ_q is θ_q, the sample score $T_o{}^s$ can be calculated by Eq. (16), from which the sample priority is observed.

$$T_o^s = \sum \xi_q \theta_q (o = 1, 2, \cdots, n; q = 1, 2, \cdots, G) \quad (16)$$

where θ_q is determined by the sortation of vectors ξ_q and the expectation of designers.

3. *CBL* evaluation using unascertained measurement theory

The violence and suddenness of coal burst is a long-standing issue that needs to be solved in an effective and efficient manner. The mechanical response of coal mass is affected by many factors, e.g., underground water and gas pressure, which are different from the factors of rock mass. *GB* was considered as an efficient methodology to assess the coal burst proneness. However, it has a weak performance in some complex cases. Consequently, unascertained measurement theory is utilized combining with synthetic weight to classify the burst potential of sample databases. The technique routine is summarized in Fig. 3. The samples are mainly derived from 12 provinces, China, e.g., Heilongjiang province, Shandong province and Shanxi province (Fig. 4), and the outliers are removed from the dataset (Table 2). It is clear that the training sample set constructed in this work is representative of the inspired amount. Four evaluation indexes (DT, W_{ET}, K_E and R_C) are investigated to realize the *CBL* classification. The index correlation and classification basis [32] are presented in Fig. 5 and Table 3.

3.1. Calculation of unascertained measurement value

In this study, another two membership functions (*S* and *W* functions) are added into the algorithm to extend the ability of uncertainty measure in addition to commonly-used linear and non-linear methodologies. Considering the complexity of underground engineering and the simplicity of linear function, the linear and non-linear evaluation regarding coal burst risks are carried out simultaneously based on the given functions to choose the hybrid model with optimal structure. The second sample is taken as an example. The single index measurement vectors (Fig. 6) are calculated based on Eqs. (1)–(4), shown in Fig. 7, which meets Eqs. (5)–(7) requirements.

3.2. Weight analysis and composite measurement

Weight calculation, which assigns more influence on the important factors, determines the accuracy of evaluation results. Subjective and objective weighting methods are performed simultaneously to promote the rationality of weight allocation. For the subjective weights, a pairwise comparison matrix is constructed by researchers based on the rich field experience. To remove the uncertainty for decision-makers during the index importance comparison as much as possible, the rating interval of 1–9 was replaced by 1–4. The eigenvectors corresponding to the maximum eigenvalue are the index weights after the consistency check is satisfied (Eqs. (11) and (12)). In this study, the subjective weighting of DT, W_{ET}, K_E and R_C are specified as {0.4673, 0.16, 0.095, 0.2772}. Besides, the commonly-used weights {0.3, 0.2, 0.2, 0.3} [37] are also applied to validate the feasibility of index

Table 3
Classification basis regarding the influential factors.

Classification	DT (ms)	W_{ET}	K_E	R_C (MPa)
ξ_1 (none)	>500	<2	<1.5	<7
ξ_2 (weak)	50–500	2–5	1.5–5.0	7–14
ξ_3 (strong)	≤50	≥5	≥5	≥14

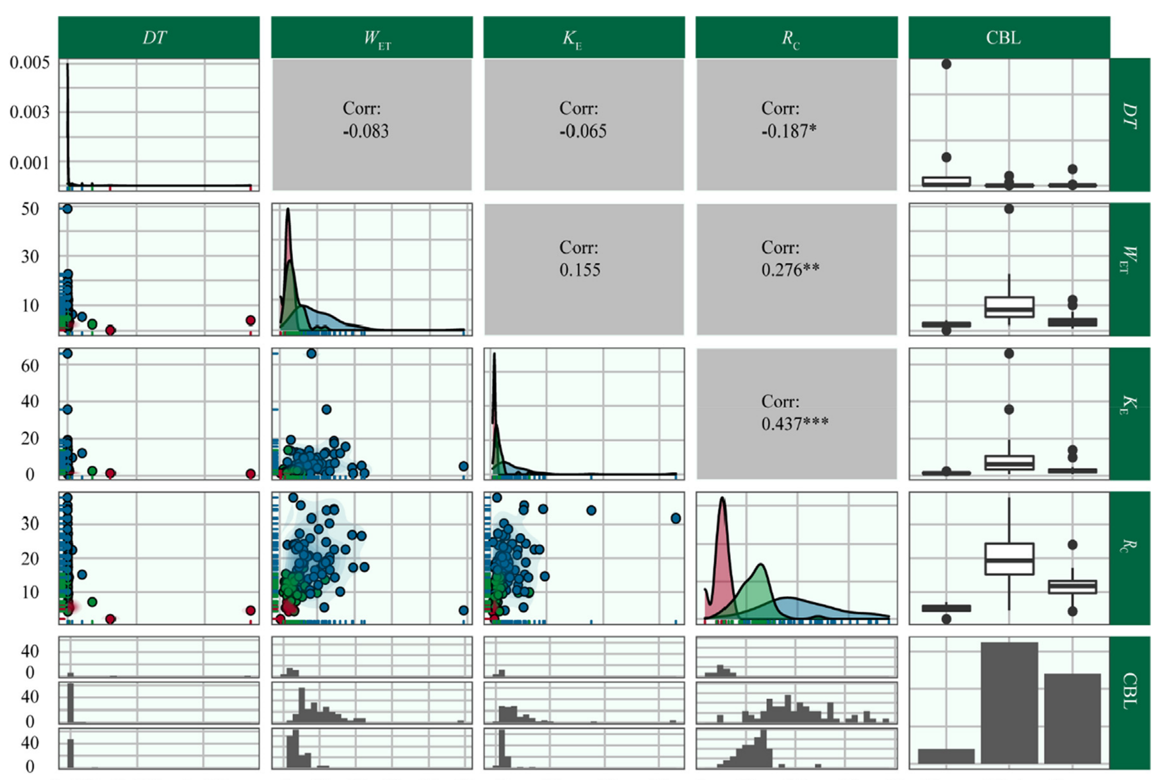

Fig. 5. Correlation matrix of *CBL* evaluation indexes.

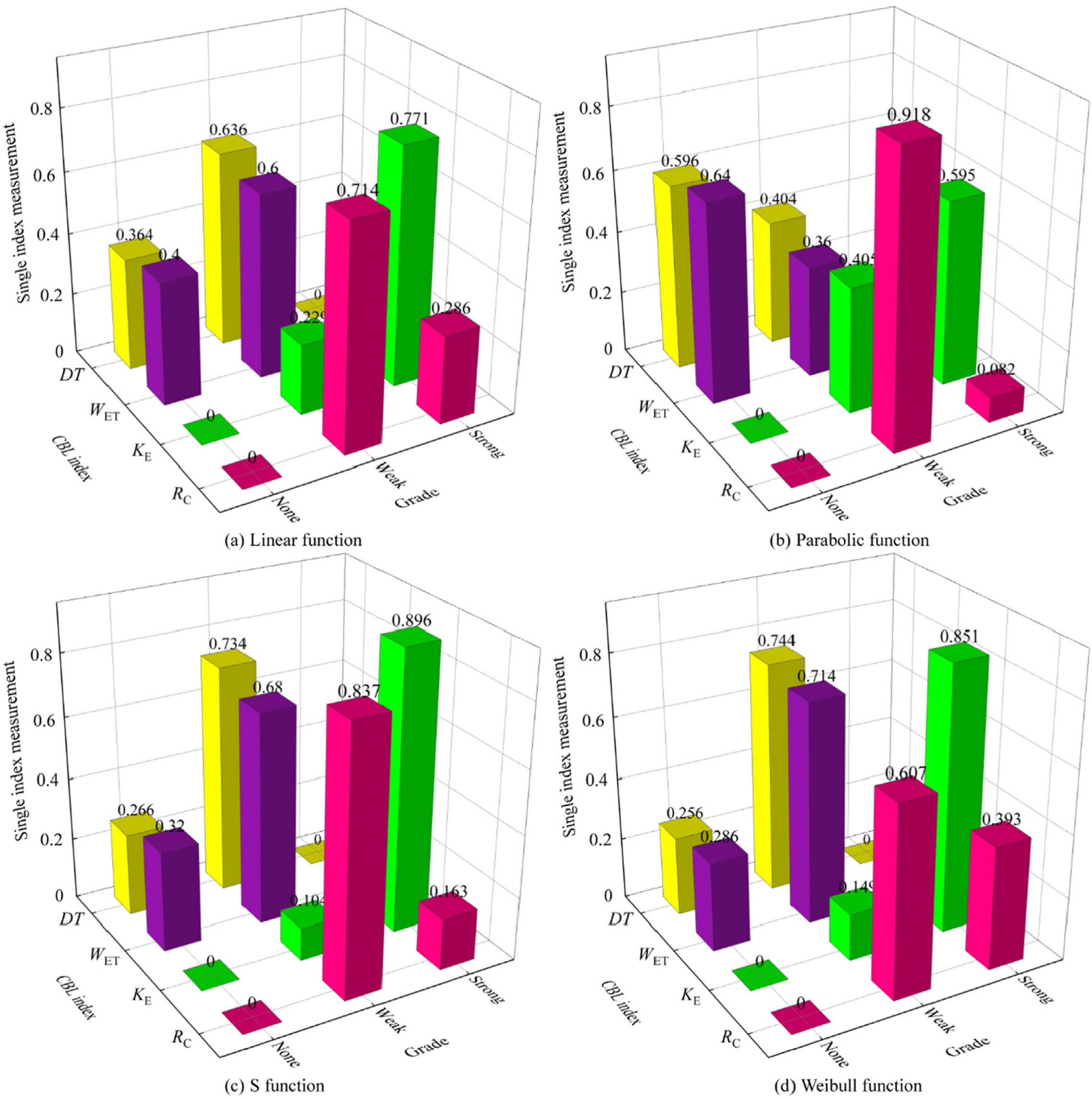

Fig. 6. Single index measurement vectors of sample (Pingdingshan sixth mine).

weight determination. Then, the synthetic weights of individual samples can be achieved according to Eq. (13), as shown in Table 4.

3.3. Composite measurement vectors and CBL classification

Sample/composite measurement is able to size the main characteristics of the object to be evaluated compared to the single index measurement. In this study, the comprehensive measurement vectors are calculated via multiple index measurement matrix and synthetic weights, see Eq. (14).

The attribute characteristic of samples can be observed clearly in the composite measurement vectors context. After that, a high-efficient attribute identification criterion is necessary, which has a capability of classifying the *CBL* reasonably. In the past, a lack of suitable division criterion leads to a low accuracy, which turns out to limit the combination model extension to other fields. Consequently, credible recognition principle is used to categorize the *CBL*, which outperforms the maximum measurement principle in ordered partition space $\mathit{\Lambda}$ [48]. The composite measurement vectors of the second sample are presented as {0.306, 0.615, 0.079} according to Eq. (15) (λ = 0.6), then, 0.306 + 0.615 > λ = 0.6, that is, the grade of the second sample is ξ_2, which corresponds to be weak in *CBL* classification. The evaluation results for the rest of the samples under different membership functions are computed as sample 2. In Fig. 8, the accuracy of different ensemble models are visualized, and the evaluation results with optimal structure are listed. The accuracy of all unascertained measurement-based ensemble models is more than 80%, which indirectly proves the reasonability of this model in *CBL* evaluation. Additionally, the evaluation performance of the optimal ensemble model is shown in Fig. 9, using a confusion matrix. It is clear that the accuracy of *P-CW-CIP* is 91%.

As noted in Fig. 8, A^* represent the index weight collected from the literature.

3.4. Priority sortation to coal burst database

The values of three grades are presented as {60, 80, 100}, according to Eq. (16). Then, the scores of individual specimen are obtained with different combination methodologies. The entire

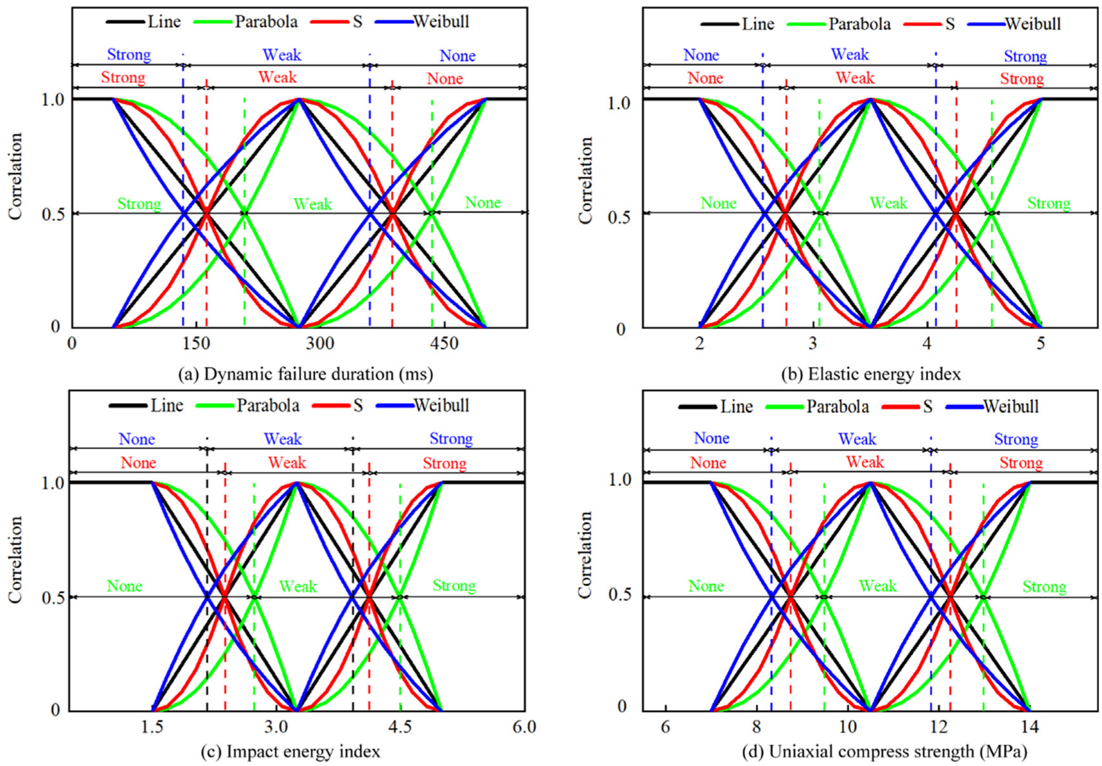

Fig. 7. Uncertainty measurement of different functions.

Table 4
Weight distribution of *CBL* evaluation parameters.

CBL parameter	*AHP*	*AHP* (*)	Entropy method				Combination weight (EN-AHP)			
			L	*P*	*S*	*W*	*L*	*P*	*S*	*W*
DT	0.4673	0.3	0.229	0.201	0.216	0.248	0.443	0.370	0.425	0.485
W_{ET}	0.16	0.2	0.221	0.211	0.196	0.234	0.146	0.133	0.132	0.157
K_E	0.095	0.2	0.291	0.201	0.317	0.317	0.114	0.075	0.127	0.126
R_C	0.2772	0.3	0.259	0.387	0.271	0.201	0.297	0.422	0.317	0.232

Note: *AHP* (*) is the subjective weight obtained from the literature [37].

scores of samples are presented below based on *P-CW-CIP* combination model (Fig. 10). The sample score and *CBL* are positively correlated, and the red and green lines shown in Fig. 10 are assumed as the boundary to classify the *CBL*. From Fig. 10, it can be said that the majority of samples (over 90%) may suffer from a different levels of coal burst hazard, from which the efficient hazard control techniques can be employed to remove this negative impact effectively.

3.5. Engineering validation with unascertained model

The *GB* plays a major role in identifying the coal burst risk for a long time, the GB principle is to judge the burst intensity comprehensively according to the evaluation of four correlative parameters. However, the results implemented by empirical criterion are ambiguous in the situation, where these indexes belong to different grades respectively. Generally, in this case other assessment outcomes which are similar to this condition are employed as a reference. In this work, 11 new coal burst samples are used to validate the reliability of the hybrid model, which is selected in section 3.3. Table 5 illustrates the coal burst parameters and its evaluation results judged with distance discriminant analysis (*DDA*) as well as *GB*. The *CBL* of all engineering cases cannot be judged by *GB* absolutely as shown in Fig. 11. Wang et al. [95] investigated the similar conditions to distinguish the intensity and to validate performance of the proposed *DDA* model. In some cases, the aforementioned comparison technique is able to improve the credibility of estimation. But the comparison sample is hard to gather, of which the attribute label is clear. The optimal combination of unascertained models is performed to classify the *CBL*. On the one hand, it is able to examine the applicability of this hybrid algorithm. On the other hand, this algorithm can also classify the species, which is hard to distinguish with *GB*, via the parameters and the corresponding division criterion. In Fig. 12, the *CBL* can be classified through the accumulative comprehensive measurement vectors and *CIP*. The evaluation results are shown in Table 5, which are perfectly consistent with the actual situation or other evaluation methods.

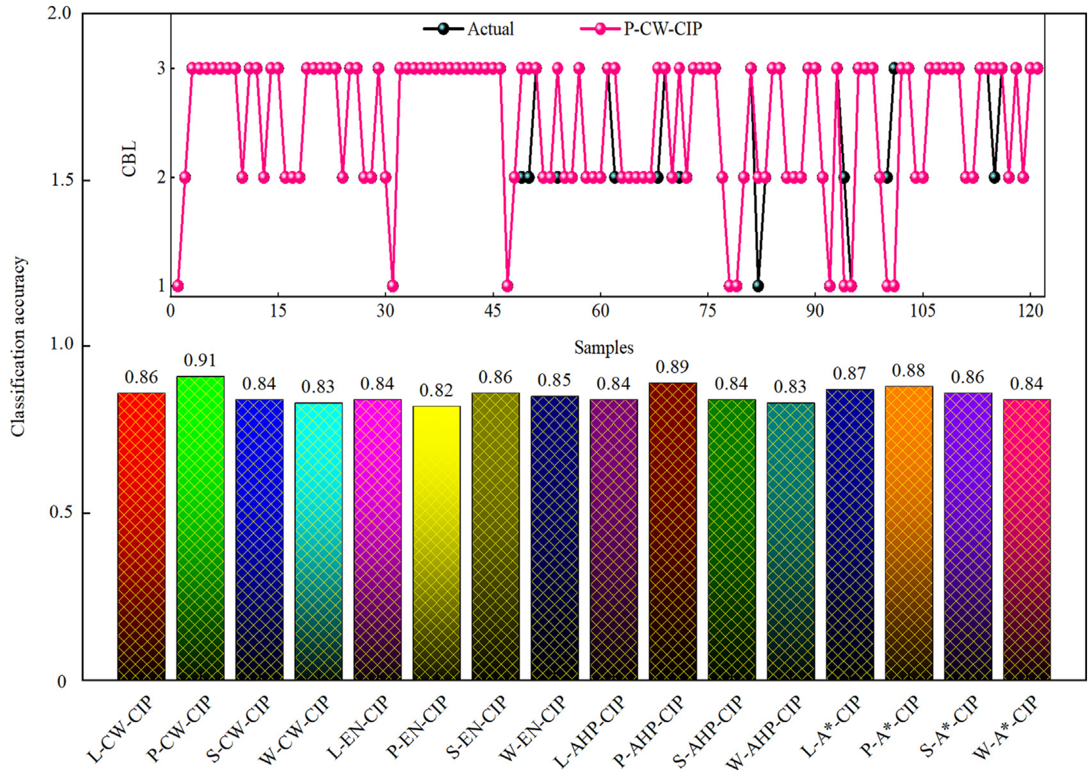

Fig. 8. Evaluation performance of different hybrid models.

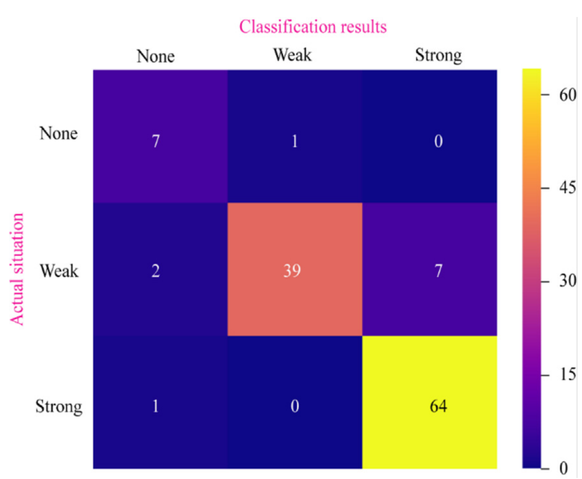

Fig. 9. Confusion matrix of the *P-CW-CIP* model.

3.6. Comparison and discussion

In previous studies, few ones focused on the process that selects an optimal model, the existing hybrid models are usually designed for possessing specific cases. In this study, a process to establish an optimal hybrid algorithm is introduced through a theoretical analysis and calculation. Entropy-based method (*EN*) can prevent the subjective disturbance of the designers, while it may result in the severely deviating weights from the actual situation. For *AHP*, the weights assignment is feasible in most of the cases, which can make full use of the rich engineering experience of designers and planners. However, the sensitivity of the index importance is different, which can generate the uncertainty factors to evaluate the results. Last but not the least, choosing a reasonable classification tool to judge the *CBL* accurately is very crucial. Usually, maximum measurement principle is not accepted in this case, and *UC* and *CIP* are considered as the common classification criteria. However, the application scope of the former is not clear and it sometimes gets unacceptable classification results. Therefore, there are 24 possible combination styles including L-EN-UC, L-EN-CIP, L-AHP-UC, L-AHP-CIP, L-CW-UC, L-CW-CIP, P-EN-UC, P-EN-CIP, P-AHP-UC, P-AHP-CIP, P-CW-UC, P-CW-CIP, S-EN-UC, S-EN-CIP, S-AHP-UC, S-AHP-CIP, S-CW-UC, S-CW-CIP, W-EN-UC, W-EN-CIP, W-AHP-UC, W-AHP-CIP, W-CW-UC and W-CW-CIP to describe the *CBL*. According to the evaluation results, it can be seen that the accuracy of all uncertainty-based hybrid models exceeds 80%. The models P-CW-CIP and P-AHP-CIP achieve the best performance (Fig. 8) with 91% and 89% accuracy, which proves that the subjective weights used in this work are reliable. Considering the ability of synthetic weights to reduce the subjective disturbance on weights assignment, this study *P-CW-CIP* hybrid model is selected as the best one to estimate the *CBL*.

For the samples, *GB* is hard to categorize, and empirical comparison seems to be an inspired way to get rid of the dilemma but it is impractical and time-consuming to search suitable case history. Thus, eleven new coal burst samples with complete intensity labels, some of which cannot be classified by *GB*, are gathered to test the performance of combination algorithm P-CW-CIP (λ = 0.6). As shown in Table 5, the evaluation results are in accordance with the field description or *GB*, through which the performance of this robust combination is validated. It means that the evaluation results obtained by unascertained measurement theory are reliable.

The unascertained measurement model considering the index importance with synthetic weight is able to evaluate the *CBL* rea-

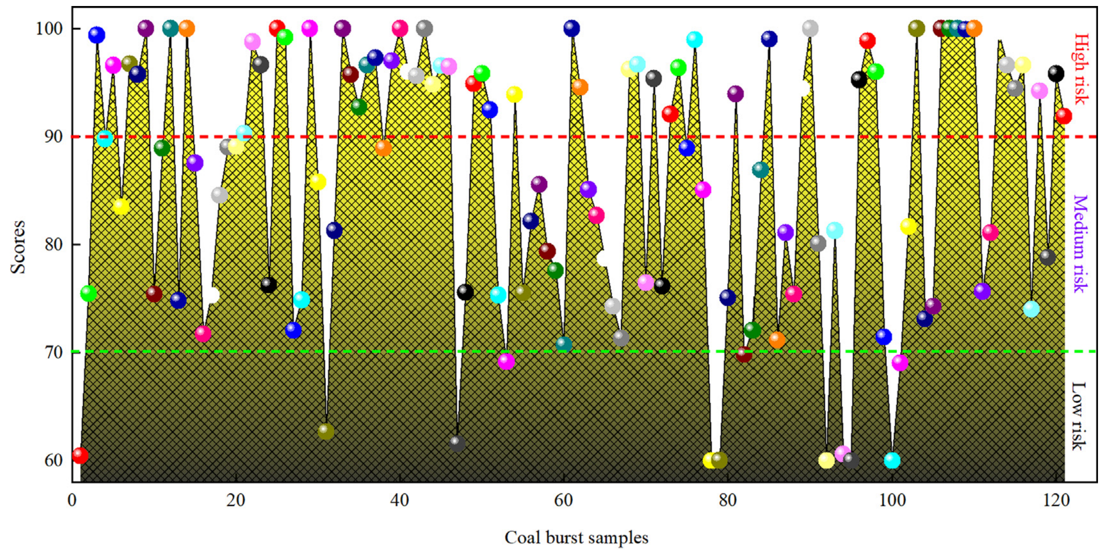

Fig. 10. CBL sortation via the specimen scores.

Table 5
Coal burst parameters adopted for model tesing.

Sample	*CBL* index				*DDA* method	GB	Actual situation	UM	Reference
	DT (ms)	W_{ET}	K_E	R_C (MPa)					
Zhaozhuang coal mine	196	1.93	1.08	8.9	Weak	*	Weak	Weak	Wang et al. (2019) [95]
Babao mine	12,333	0.96	1.14	4.56	None	None	None	None	
Sanhejian coal mine	70	7.83	3.38	20.8	Strong	*	Strong	Strong	
Datong mine	318	3.6	0.9	0.7	None	*	None	None	
Fuxing mine	142	0.116	2.22	1.68	None	*	None	None	
Lingzhida mine #15	1336	1.98	1.47	8.03	–	None	–	None	Niu et al. (2021) [96]
A mine 3 level	535.75	3.11	3.23	5.57	–	None	–	None	Du (2020) [97]
Baoan mine #15	889	1.89	1.73	6.47	–	None	–	None	Zhao (2020) [98]
Tangkou mine LW5304 (10 d)	30	3.38	6.48	13.97	–	Strong	Strong	Strong	Liu et al. (2018) [99]
Tangkou mine LW5304 (20 d)	134	3.09	1.42	13.5	–	Weak	Weak	Weak	
Tangkou mine LW5304 (30 d)	160	2.62	1.51	10.36	–	Weak	Weak	Weak	

Notes: – represents that the *CBL* hasn't been evaluated through *DDA* method; and * represents the cases that cannot be divided by *GB*.

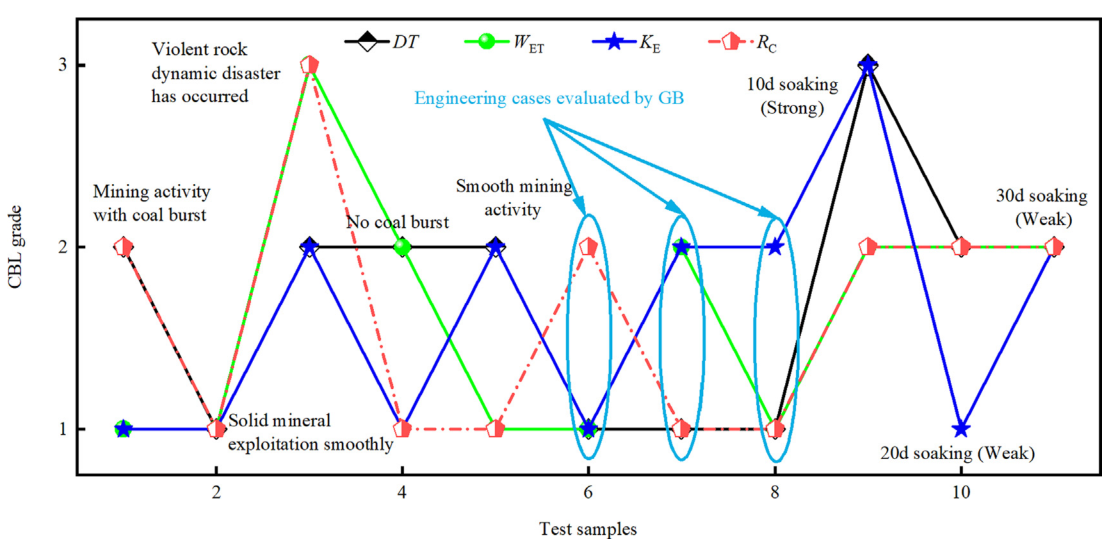

Fig. 11. Discriminant results of individual index using *GB*.

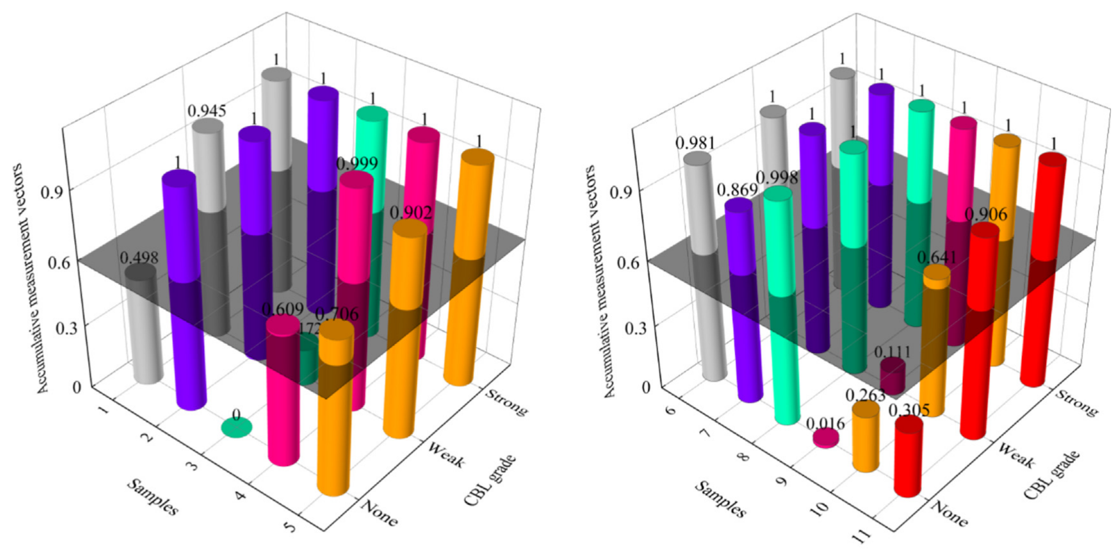

(a) The composite measurement of samples 1~5

(b) The composite measurement of samples 6~11

Fig. 12. The accumulation of composite measurement vectors of 11 samples.

sonably, and the advantages of this model in comparison with other researches are summary below:

(1) Different from conventional mechanism research, P-CW-CIP is able to efficiently interpret valuable information, e.g., *CBL*, through the on-site data, which is also the development tendency of the future. On the one hand, various coal burst proneness corresponds to the different levels of characteristic parameters; on the other hand, a large volume of monitoring techniques that are undisturbed to coal mass provide the possibility of constructing a data-based algorithm. Several uncertainty evaluation algorithms have been developed and improved by many scholars in recent years, e.g., fuzzy evaluation is able to deal with fuzzy uncertainty information, which also suffers from the loss of valuable information. Compared to fuzzy evaluation, it seems that unascertained measurement theory gains more attention to deal with uncertainty information based on its principle (normalization, non-negativity and additivity). Therefore, the developed model is capable of assessing the *CBL* in a safe environment on the basis of the inspired coal burst dataset compared to on-site tests. More importantly, the structure of the proposed model is simple, which is beneficial to be accepted in engineering.

(2) The number of specimens is not the main limit of this algorithm compared to the statistics method, that is, the evaluation result is still reliable in the case of small samples. For the structure of the proposed model, employing multiple non-linear membership functions can remove the uncertainty information existing in the engineering problems as much as possible. As aforementioned, both subjective and objective weights have their limitations. Thus, the weighted mean method, which considers the proportion distribution of different weights at the same time, is utilized to measure the index importance comprehensively. Furthermore, the weight is calculated based on the multiple index matrix, that is, the sample difference is highlighted in this model (each sample ψ_i corresponds to a weight ω_p). In this way, the determination of weight is more scientific, which can be validated through the evaluation accuracy shown in Fig. 8.

In engineering projects, many uncertainty factors contribute to the coal burst hazard, yet the current comprehensive evaluation methods are far from the engineering requirements. The proposed model shows a great potential in this field, but, the index system used is based on the previous researches, which leads to other important influencing indicators, for example, geo-stress is not explored, and the index sensitivity is not taken into account. Besides, the method to determine the value of *CIP* is from literature, as a result, the criterion selection may suffer from the artificial disturbance for special engineering cases. Therefore, other classic algorithms, e.g., set pair analysis, will be incorporated in the next research through which the proposed model can be further optimized.

4. Conclusions

In this paper, 121 groups coal burst data and 11 groups test samples are constructed to select the optimal combination model, and the performance of the established model is tested separately. The indexes (DT, W_{ET}, K_E and R_C) are determined as the input variables of the targeted models. Multiple-index measurement matrix and weights distributions are calculated based on the dataset, then credible identification principle (λ = 0.6) is performed to classify the *CBL* explicitly. The results show that the uncertainty-based model performs well in *CBL* analysis, which means that it can be seen as a supplement of conventional disaster evaluation methods.

(1) Two new non-linear membership functions (*S* and *W*) are created to quantify the uncertainty as it belongs to different classes simultaneously in addition to conventional linear and non-linear assessment approaches. Then, synthetic weights are employed to investigate the weights of individual indexes, which is able to incorporate the advantages of information entropy and *AHP* method.

(2) The subjective weights of index system are presented as {0.467, 0.16, 0.095, 0.277}, then, the combination models L-EN-UC, L-EN-CIP, L-AHP-UC, L-AHP-CIP, L-CW-UC, L-CW-CIP, P-EN-UC, P-EN-CIP, P-AHP-UC, P-AHP-CIP, P-CW-UC, P-CW-CIP, S-EN-UC, S-EN-CIP, S-AHP-UC, S-AHP-CIP, S-CW-UC, S-CW-CIP, W-EN-UC, W-EN-CIP, W-AHP-UC, W-AHP-CIP, W-CW-UC and W-CW-CIP are established via analyzing correlative part of the targeted model. The evaluation results show that the accuracy of established models exceeds 80%, and the ensemble model P-CW-CIP (λ = 0.6) shows the best

performance with 91% accuracy. Additionally, more than 90% samples of training dataset are at the risk of coal burst according to the sample superiority sortation. As for the test sample, the P-CW-CIP model shows great potential in CBL classification with 100% accuracy.

(3) In this work, other important influencing factors, e.g., geo-stress, is not explored for the CBL evaluation. Meanwhile, the method used for identifying the most essential factors in CBL evaluation is not explored. Thus, these limitations need to be overcome in the next research.

Acknowledgements

This research was funded by the National Science Foundation of China (Nos. 72088101 and 41807259), the Innovation-Driven Project of Central South University (No. 2020CX040) and the Shenghua Lieying Program of Central South University (Principle Investigator: Dr. Jian Zhou).

References

[1] Li XB, Zhou J, Wang SF, Liu B. Review and practice of deep mining for solid mineral resources. Chinese J Nonferrous Metals 2017;27(7):1236–62.
[2] Ouyang Z, Zhang G, Li Q, Lai X, Qin H, Zhao X, Zhou X. Study on the rock burst tendentiousness of coal under different gas pressures. Arabian J Geosci 2020;13(1):1–13.
[3] Cai W, Dou L, Si G, Cao A, Gong S, Wang G, Yuan S. A new seismic-based strain energy methodology for coal burst forecasting in underground coal mines. Int J Rock Mech Min Sci 2019;123:104086.
[4] Wu Y, Gao F, Chen J, He J. Experimental study on the performance of rock bolts in coal burst-prone mines. Rock Mech Rock Eng 2019;52(10):3959–70.
[5] Feng J, Wang E, Huang Q, Ding H, Zhang X. Experimental and numerical study of failure behavior and mechanism of coal under dynamic compressive loads. Int J Min Sci Technol 2020;30(5):613–21.
[6] Zhou J, Li X, Mitri HS. Comparative performance of six supervised learning methods for the development of models of hard rock pillar stability prediction. Nat Hazards 2015;79(1):291–316.
[7] Shukla R, Khandelwal M, Kankar PK. Prediction and assessment of rock burst using various meta-heuristic approaches. Min, Metallurgy Exploration 2021;38(3):1375–81.
[8] Zhou J, Li X, Mitri HS. Evaluation method of rockburst: state-of-the-art literature review. Tunn Undergr Space Technol 2018;81:632–59.
[9] Gong F, Wang Y, Wang Z, Pan J, Luo S. A new criterion of coal burst proneness based on the residual elastic energy index. Int J Min Sci Technol, 2021, in press.
[10] Zhou J, Shi XZ, Dong L, Hu HY, Wang HY. Fisher discriminant analysis model and its application for prediction of classification of rockburst in deep-buried long tunnel. J Coal Sci Eng 2010;16(2):144–9.
[11] Frith R, Reed G, Jones A. A causation mechanism for coal bursts during roadway development based on the major horizontal stress in coal: Very specific structural geology causing a localised loss of effective coal confinement and newton's second law. Int J Min Sci Technol 2020;30(1):39–47.
[12] Hao X, Du W, Zhao Y, Sun Z, Zhang Q, Wang S, Qiao H. Dynamic tensile behaviour and crack propagation of coal under coupled static-dynamic loading. Int J Min Sci Technol 2020;30(5):659–68.
[13] Su C, Qiu J, Wu Q, Weng L. Effects of high temperature on the microstructure and mechanical behavior of hard coal. Int J Min Sci Technol 2020;30(5):643–50.
[14] Ning J, Wang J, Tan Y, Xu Q. Mechanical mechanism of overlying strata breaking and development of fractured zone during close-distance coal seam group mining. Int J Min Sci Technol 2020;30(2):207–15.
[15] Song D, He X, Wang E, Li Z, Wei M, Mu H. A dynamic ejection coal burst model for coalmine roadway collapse. Int J Min Sci Technol 2019;29(4):557–64.
[16] Wang S, Li L, Cheng S, Yang J, Jin H, Gao S, Wen T. Study on an improved real-time monitoring and fusion prewarning method for water inrush in tunnels. Tunn Undergr Space Technol 2021;112:103884.
[17] Yang X, Ren T, He X. Experimental study of coal burst risk prediction using fractal dimension analysis of AE spatial distribution. J Appl Geophys 2020;177:104025.
[18] Cai Wu, Dou L, Zhang M, Cao W, Shi J-Q, Feng L. A fuzzy comprehensive evaluation methodology for rock burst forecasting using micro-seismic monitoring. Tunn Undergr Space Technol 2018;80:232–45.
[19] Yardimci AG, Karakus M. A new protective destressing technique in underground hard coal mining. Int J Rock Mech Min Sci 2020;130:104327.
[20] Guo W-Y, Tan Y-L, Yang Z-L, Zhao T-B, Hu S-C. Effect of saturation time on the coal burst liability indexes and its application for rock burst mitigation. Geotech Geol Eng 2018;36(1):589–97.
[21] Zhou J, Li X, Mitri HS. Classification of rockburst in underground projects: comparison of ten supervised learning methods. J Comput Civil Eng 2016;30(5):04016003.
[22] Małkowski P, Niedbalski Z. A comprehensive geomechanical method for the assessment of rockburst hazards in underground mining. Int J Min Sci Technol 2020;30(3):345–55.
[23] Zhou J, Shi X, Huang R, Qiu X, Chen C. Feasibility of stochastic gradient boosting approach for predicting rockburst damage in burst-prone mines. Trans Nonferrous Metals Soc China 2016;26(7):1938–45.
[24] Farhadian H. A new empirical chart for rockburst analysis in tunnelling: Tunnel rockburst classification (TRC). Int J Min Sci Technol 2021, in press.
[25] Zhou J, Guo H, Koopialipoor M, Armaghani DJ, Tahir MM. Investigating the effective parameters on the risk levels of rockburst phenomena by developing a hybrid heuristic algorithm. Eng. Comput. 2020;1–16.
[26] Zhou J, Koopialipoor M, Li E, Armaghani DJ. Prediction of rockburst risk in underground projects developing a neuro-bee intelligent system. Bull Eng Geol Environ 2020;79(8):4265–79.
[27] Wasilewski S. Gas-dynamic phenomena caused by rock mass tremors and rock bursts. Int J Min Sci Technol 2020;30(3):413–20.
[28] Zhou J, Li X, Shi X. Long-term prediction model of rockburst in underground openings using heuristic algorithms and support vector machines. Saf Sci 2012;50(4):629–44.
[29] Yang Z, Liu C, Zhu H, Xie F, Dou L, Chen J. Mechanism of rock burst caused by fracture of key strata during irregular working face mining and its prevention methods. Int J Min Sci Technol 2019;29(6):889–97.
[30] Wei C, Zhang C, Canbulat I, Cao A, Dou L. Evaluation of current coal burst control techniques and development of a coal burst management framework. Tunn Undergr Space Technol 2018;81:129–43.
[31] Sabapathy R, Paul PS, Mandal PK. Evaluation of bump-proneness of underground coal mines using burst energy coefficient. Arabian J Geosci 2019;12(18):1–16.
[32] GB/T 25217.2-2010. Classification and laboratory test method on bursting liability of coal. Beijing: Standards Press of China; 2010.
[33] Manoj K, M. M. Prediction of flyrock in open pit blasting operation using machine learning method. Int J Min Sci Technol 2013;23(3):313–6.
[34] Khandelwal M, Marto A, Fatemi SA, Ghoroqi M, Armaghani DJ, Singh TN, Tabrizi O. Implementing an ANN model optimized by genetic algorithm for estimating cohesion of limestone samples. Eng Comput 2018;34(2):307–17.
[35] Wang M, Shi X, Zhou J. Charge design scheme optimization for ring blasting based on the developed Scaled Heelan model. Int J Rock Mech Min Sci 2018;110:199–209.
[36] Li E, Zhou J, Shi X, Armaghani D, Yu Z, Chen X, Huang P. Developing a hybrid model of slap swarm algorithm-based support vector machine to predict the strength of fiber-reinforced cemented paste backfill. Eng Comput 2020:1–22.
[37] Cai W, Dou L, Si G, Cao AY, He J, Liu S. A principal component analysis/fuzzy comprehensive evaluation model for coal burst liability assessment. Int J Rock Mech Min Sci 2016;100(81):62–9.
[38] Wang G, Gong S, Li Z, Dou L, Cai W, Mao Y. Evolution of stress concentration and energy release before rock bursts: two case studies from Xingan coal mine, Hegang,China. Rock Mech Rock Eng 2016;49(8):3393–401.
[39] Mark C. Coal bursts in the deep longwall mines of the United States. Int J Coal Sci Technol 2016;3(1):1–9.
[40] Wang G. Mathematics treatment of unascertained information. J Civ Eng Instit Harbin 1990;23(4):1–9.
[41] Zhou J, Li X-B. Integrating unascertained measurement and information entropy theory to assess blastability of rock mass. J Central South Univ 2012;19(7):1953–60.
[42] Zhou J, Chen C, Khandelwal M, Tao M, Li C. Novel approach to evaluate rock mass fragmentation in block caving using unascertained measurement model and information entropy with flexible credible identification criterion. Eng Comput 2021;1–21.
[43] Saaty TL. A scaling method for priorities in hierarchical structures. J Math Psychol 1977;15(3):234–81.
[44] Chen C, Zhou J, Zhou T, Yong W. Evaluation of vertical shaft stability in underground mines: comparison of three weight methods with uncertainty theory. Nat Hazards 2021;1–13.
[45] Dong L, Shu W, Li X, Zhang J. Quantitative evaluation and case studies of cleaner mining with multiple indexes considering uncertainty factors for phosphorus mines. J Cleaner Prod 2018;183:319–34.
[46] Zhou J, Chen C, Du K, Armaghani DJ, Li CQ. A new hybrid model of information entropy and unascertained measurement with different membership functions for evaluating destressability in burst-prone underground mines. Eng Comput 2020:1–19.
[47] Zhou J, Chen C, Armaghani DJ, Ma SY. Developing a hybrid model of information entropy and unascertained measurement theory for evaluation of the excavatability in rock mass. Eng Comput 2020:1–24.
[48] Chen Q. Attribute recognition theoretical model worth application. Acta Scientiarum Naturalium Universitatis Pekinensis 1997;33:12–20.
[49] Shi X, Zhou J, Dong L, Hu H, Wang H, Chen S. Application of unascertained measurement model to prediction of classification of rockburst intensity. Chinese J Rock Mech Eng 2010;29:2720–7.

[50] Luo H, Yu JK, Pan YS, Wang JL, Zhang Y. Electric charge induction law of coal rock containing gas with bursting tendency during loading failure process. J China Coal Soc 2020;45(2):684–94.

[51] Wang C, Li YF, Zhang CL, Liu L, Huang XC. Study on influence of indicator dimensionless on classification model of coal's bursting liability. China Saf Sci J 2019;29(11):20–5.

[52] Gao B, Wang Z, Li H, Su C. Experimental study on the effect of outburst-proneness of coal by gas pressure. J China Coal Soc 2018;43(S1):140–8.

[53] Pan JF, Jian JF, Liu SH, Zhang WG, Yuan DS, Wang HT, Liu H. Geological characteristic and control of rock burst of Huanglong Jurassic coal mine field. Coal Min Technol 2019;24(1):110–5.

[54] Wu GH, Wang W, Xu YG, Yang J. Experimental study on the burst tendency of extra thick seam in Hujiahe Coal Mine. ShaanxiCoal 2015;34(5). 9–11+27.

[55] Cao MY, Sun XL, Yang L, Liu YH. Study on rock burst risk assessment of fully-mechanized top coal caving mining face in steep coal seam. Coal Sci Technol 2019;47(2):47–52.

[56] Zhu ST, Jiang FX, Wang XY, Jiang YW, Ning TZ, Sun SH. Energy accumulation characteristics and rockburst mechanism of surrounding rock at heading face of extra-thick coal seam. Chinese J Geotechnical Eng 2019;41(11):2071–8.

[57] Wang LF, Zhong ZH, Liu YL, Xin CR. Evaluation and Control of rock Burst Hazard of 2315 Working Face of Anju Coal Mine. Coal Min Technol 2019;24(1):120–3.

[58] Wang G, Pan Y, Xiao X. Experimental study on influence of burst tendency on damage charge law of coal sample under loading. Coal Sci Technol 2019;47(11):247–54.

[59] Li PB, Wang JA. Application of principal component analysis in coal rockburst tendency in judgment. Coal Technol 2016;35(3):19–21.

[60] Guo JD. Application of variable weight and grey classification recognition model in rock burst tendency evaluation of coal seam. J North China Instit Sci Technol 2017;14(1):44–9.

[61] Li GF. Study on rockburst risk zone division and control technology in Pingdingshan coal industry group NO.4 coal mine Master dissertation. Jiaozuo: Henan Polytechnic University; 2011. p. 24–37.

[62] Bai ZQ. Experimental study on impact mechanics of deep coal and rock. Technol Wind 2018;30:4.

[63] Su CD, Yuan RF, Zhai XX. Experimental research on bursting liability index of coal samples of Chengjiao coal mine. Chinese J Rock Mech Eng 2013;32(S2):3696–704.

[64] Li Y, Zhang YY, Huang YQ, Liu JX. Analysis on Inducing Factors of "7.15" Rock Burst Accident in Chengshan Mine. Nonferrous Metal Eng 2013;3(3):53–6.

[65] Song LS, Zhao SK, Liu J, Wei XZ, Han RJ, Jiang HB. Experimental research on rules of rock burst tendency evolution and mechanical properties of "roof-coal"structure body. J China Coal Soc 2014;39(S1):23–30.

[66] Wan CX. Effect of different moisture state on coal bursting tendency. Opencast Min Technol 2015;2:31–5.

[67] Gong HG, Fan JP, Li Q, Pang JL, Sun ZP, Zhang CC. Prevention study on mining dangerous zone with weak outburst proneness and complicated conditions. Saf Coal Mines 2015;46(7):51–4.

[68] Wang J, Cun JS, Hao YX, Zhang YL, Meng ZG, Wang H. Experimental study on bursting liability of 12# coal and roof rock of Hongyang coal mine. China Mining Magazine 2016;25(5):70-3+101.

[69] Su CD, Gao BB, Yuan RF, Yang J. Outburst-proneness index and their correlation analysis of coal seams in Pingdingshan mine area. J China Coal Soc 2014;39(S1):8–14.

[70] Li BF. Study on burst tendency differentiation index of 2# coal seam in Qianqiu coal mine. J Saf Sci Technol 2014;10(5):62–7.

[71] Zhang PD, Cui JS, Wang H, Cai F, Gao C. Test Study on the impact tendency of No. 7 coal and roof in Yaoqiao coal mine. Coal Sci Technol Mag 2015;3:47–50.

[72] Shu YM, Liu YL, Qin T. Bump proneness determination and analysis of coalseam in Xinxing mine. Value Eng 2014;33(20):51–2.

[73] Yang L. The acoustic emission characteristics of rockburst tendency coal sample in the destruction process. Master dissertation. Beijing: China Coal Research Institute CCRI 2013:23–4.

[74] Xu ZJ. Study on AE and infrared radiation laws of coal damage evolution under uniaxial compression Master dissertation. Fuxin: Liaoning Technical University; 2013.p.20..

[75] Li HY, Kang LJ, Xu ZJ, Qi QX, Zhao SK. Precursor information analysis on acoustic emission of coal with different outburst proneness. J China Coal Soc 2014;39(2):384–8.

[76] Guo GH. Comprehensive prevention and control measures of rock burst in Yuejin coal mine of Yimei coal company. Coal Sci Technol Mag 2016;1:115–7.

[77] Tong YN. Research on rockburst risk of working face in the Zhaozhuang mine Master dissertation. Fuxin: Liaoning Technical University; 2014.p.25..

[78] Xing LJ. Research on the characteristic and control technology of rock burst under the condition of deep mining and hazard roof. Xi'an: Xi'an University of Science & Technology; 2014.p.22..

[79] Li ZY. Research on the law of mine seismic in impact dangerous face. Energy Technol Manage 2013;38(4):21–3.

[80] Wang WJ. Research on the impact mechanism of coal seam burst tendency on rock burst Doctoral dissertation. Beijing: China University of Mining and Technology; 2013.p.28..

[81] Song YF, Pan YS, Bao SY. Study on electric charge induction during bump proneness coal failure process. China Saf Sci J 2018;28(2):151–7.

[82] Jiang JJ, Deng ZG, Zhao SK, Li HT, Liu YT. Discussion on dynamic response mechanism of dynamic load-induced unloading coal. Coal Science and Technology 2018;46(7):41-7+92.

[83] Zhan ZW, Shen JB, Cai KQ. Simulation analysis of water injection effect in coal seam with strong shock tendency. Modern Min 2018;34(2):208–10.

[84] Xiao XC, Jin C, Ding X, Pan YS. Experimental study on rock burst tendency of coal with different moisture content based on acoustic emission time-frequency signals. J China Coal Soc 2018;43(4):931–8.

[85] Shen ZL, Jiang YN. Parameters analysis on strong bumping coal AE characteristics under recycled load. Shanxi Architechture 2016;42(19):49–50.

[86] Chen YT. Study on risk assessment and depressurization technology of bump rock in the thick coal seam mining kilometers of coal mine. Master dissertation. Handan: Hebei University of Engineering; 2015;14.

[87] Liu JH, Wei ZY, Wei ZQ, Shen W. Danger analysis and prevention and control technology of strata pressure bump occurred in coal pillar zone of deep mine. Coal Sci Technol 2014;42(12):41–4.

[88] Zhu MM, Liang XC, Ren Y. Test and prevention measures of burst potential in deep well. Jiangxi Coal Sci Technol 2013;3:137–40.

[89] Liu CG. The percussive test research of recycling coal strata for mining pillar in Tongjialiang coal. J Taiyuan Univ Technol 2011;42(3):252–4.

[90] Wang GF, Li Q, Zhao ZL, Pang YH. The impact tendentiousness testing of working faces and roadways with strong rock burst and force support system. J Shandong Univ Sci Technol 2011;30(4):1–9.

[91] Jiang CL, Jiang ZQ, Zhang R. Experimental study of impact proneness of deep coal seam and roof rock. Coal Technol 2010;29(9):108–10.

[92] Jiao ZY, Wang LY. Research on impact tendentiousness in D6 coal seam in No.1 coal mine of Pingdingshan coal industry comp. Coal Technology 2010;29(4):74–6.

[93] Guo DM, Hou JF, Yan HX, Wang J, Cheng HY, Wang YX. Research on rockburst tendency and its preventive measures of -1300m deep surrounding rock in Suncun coal mine. J Jiaozuo Instit Technol (Nat Sci) 2003;1:9–11.

[94] Li H, Qi S, Dai RZ. Burst-prone experiments of deep underground coal in Chaoyang coal mine. Saf Coal Mines 2008;07:11–4.

[95] Wang C, Song D, Zhang C, Liu L, Zhou Z, Huang X. Research on the classification model of coal's bursting liability based on database with large samples. Arabian J Geosci 2019;12(13):1–10.

[96] Niu WJ, Wang C, Liang H. Research on the tendency of coal and rock impact of 15# coal seam in Lingzhida Mine. Energy Technol Manage 2021;46(1):46–8.

[97] Du Z. Test and analysis of coal and rock shock tendency in a coal mine. Modern Min. 2020;36(4). 212–5,21.

[98] Zhao SW. Experimental study on No.15 coal seam impact tendency of Babao coal mine in Yangquan mining area. Energy Energy Conservation 2020;11:6–13.

[99] Liu Z, Cao A, Guo X, Li J. Deep-hole water injection technology of strong impact tendency coal seam-a case study in Tangkou coal mine. Arabian J Geosci 2018;11(2):1–9.

[101] Zhou J, Shen X, Qiu Y, Li E, Rao D, Shi X. Improving the efficiency of microseismic source locating using a heuristic algorithm-based virtual field optimization method. Geomech Geophys Geo-Energy Geo-Resour 2021.

[102] Zhou J, Qiu Y, Khandelwal M, Zhu S, Zhang X. Developing a hybrid model of Jaya algorithm-based extreme gradient boosting machine to estimate blast-induced ground vibrations. International Journal of Rock Mechanics and Mining Sciences 2021;145:104856.

[103] Khandelwal M, Singh TN. Prediction of blast-induced ground vibration using artificial neural network. International Journal of Rock Mechanics and Mining Sciences 2009;46(7):1214–22.